

## Sensing characteristics and surface reaction mechanism of alcohol sensors based on doped SnO<sub>2</sub>

Hae-Won Cheong and Man-Jong Lee\*

Agency for Defense Development, Youseong P.O. Box 35, Daejeon 305-600, Korea

Using gas chromatographic analyses, the effects of additives (PdCl<sub>2</sub>, Al<sub>2</sub>O<sub>3</sub>, and La<sub>2</sub>O<sub>3</sub>) on the alcohol-sensing properties of SnO<sub>2</sub>-based sensor elements were investigated. Also, the decomposition products of the alcohol gases and their decomposition steps at the surface of the SnO<sub>2</sub>-based powder elements were analyzed. Ethanol was catalytically oxidized by the SnO<sub>2</sub>-based powders. With the PdCl<sub>2</sub>-doped SnO<sub>2</sub>, the C-C bond cleavage product, methane, was produced. This seems to be related with the significant promotional role of PdCl<sub>2</sub>-doping in the sensing of ethanol, especially at temperatures below 300 °C. With the La<sub>2</sub>O<sub>3</sub>-doped SnO<sub>2</sub>, relatively large amounts of CO and CO<sub>2</sub> were produced, resulting in an enhanced sensitivity. On the other hand, with the Al<sub>2</sub>O<sub>3</sub>-doped SnO<sub>2</sub>, selective dehydration, which consumes the less adsorbed oxygen species (O<sub>ads</sub><sup>-</sup>), seems to degrade the sensitivity. When exposed to methanol, the SnO<sub>2</sub>-based sensors showed oxidation products consisting of CO, CO<sub>2</sub> and H<sub>2</sub>O and sensing characteristics similar to those seen with ethanol.

**Key words:** Gas sensor, SnO<sub>2</sub>, Alcohol sensing, Gas chromatography, Reaction step, Dopant.

### Introduction

With the emerging importance in the detection of toxic and flammable gases, the significance of gas sensing in military and industrial applications has been emphasized. In this area, tin oxide (SnO<sub>2</sub>) sensor material has been widely applied as a basic material in gas sensors primarily due to its high sensitivity and low cost [1]. Alcohol vapor has been one of the most extensively studied gases for these sensors [2-4], particularly due to the need for portable practical devices to detect alcohol on the human breath or to detect leaks in distribution lines of industry.

In SnO<sub>2</sub> sensors, the gas sensing mechanism can be described in terms of an adsorption/desorption process of oxygen at the surface of a sensing element. Thus, for the complete description of sensor response, the interactions between the sensor element and the target gas should be clarified. The reaction mechanism of alcohol detection by tin oxide films was extensively investigated to understand the nature of alcohol gas detection. In particular, Ogawa et al. [5], Kohl [8] and Rao et al. [6] reported the interaction of ethanol vapor with a SnO<sub>2</sub> surface. Using thermal desorption spectroscopy (TDS), Kohl and coworkers [7-9] investigated the desorption of intact ethanol, acetaldehyde, ethylene, and water from an SnO<sub>2</sub> (110) face after exposing it to ethanol. These decomposition products, along with the

resulting hydrogen donors and the surface donors, have been proposed to be responsible for a resistance change. Additives, such as metal oxides, are known to improve the sensitivity and selectivity of SnO<sub>2</sub> sensors. The acidic Al<sub>2</sub>O<sub>3</sub> and basic La<sub>2</sub>O<sub>3</sub> additives are known to improve the sensitivity to CO and ethanol, respectively [10, 11]. Catalysts [12, 13] such as a palladium are also known to enhance the sensitivity at lower operating temperatures. However, the detailed effect of catalysts on the decomposition reaction steps of alcohol gases has not been clarified up to now to the best of authors' knowledge.

For a comprehensive understanding of the detailed gas-sensing mechanism, it is desirable to identify the detailed decomposition reaction steps of the target gases at the surface of sensing elements. Thus, in this paper, based on the decomposition studies using gas chromatography (GC), we tried to clarify the detailed reaction mechanisms between the target gas and the SnO<sub>2</sub> sensor element doped with PdCl<sub>2</sub>, La<sub>2</sub>O<sub>3</sub> or Al<sub>2</sub>O<sub>3</sub>. Furthermore, we investigated the effects of different additives on the gas sensing properties.

### Experimental Procedure

#### Sample preparation

The SnO<sub>2</sub> (Aldrich, 99.9%, < 325 mesh) base material was mixed mechanically with additives such as PdCl<sub>2</sub> (0.25-1.0 wt%), Al<sub>2</sub>O<sub>3</sub> (2.0 wt%) or La<sub>2</sub>O<sub>3</sub> (5 wt%) followed by calcination in air at 600-850 °C for 2 h. The calcined powders were ball-milled for 12 h with ethanol and were dried at 80 °C in an oven. For comparison, the undoped SnO<sub>2</sub> powder was prepared

\*Corresponding author:  
Tel : +82-42-821-2019  
Fax: +82-42-823-3400  
E-mail: manjonglee@dtaq.re.kr

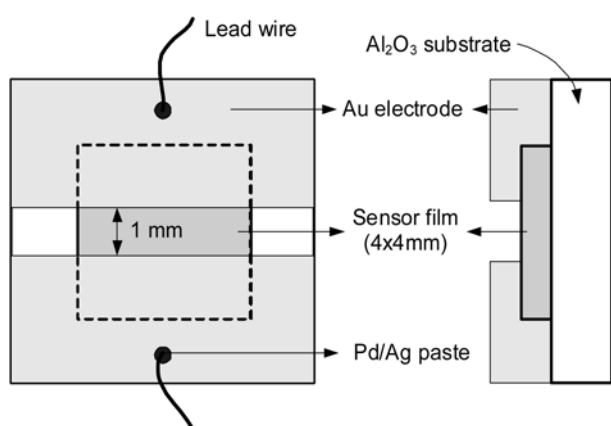


Fig. 1. Schematic diagram of a thick-film gas sensor.

by ball milling alone, *i.e.*, without calcination. The ball-milled powders were mixed with an aqueous solution of polyvinyl alcohol and the resulting pastes were screen-printed on alumina substrates. After drying, the thick films were sintered at 650–800 °C for 1 hour, except for the Al<sub>2</sub>O<sub>3</sub>-doped SnO<sub>2</sub> thick film, which was sintered at 800 °C for 2 hours. The heating and cooling rates were 10 K·minute<sup>-1</sup> and 5 K·minute<sup>-1</sup>, respectively. As electrodes, gold was sputter-deposited on the surface of the thick film except for 1 mm wide strip in the middle as shown in Fig. 1. To reduce the contact resistance, a Pd/Ag paste was applied on top of the gold electrodes. All the sensors were pretreated at 300 °C for 72 hours before measuring the gas sensitivity.

### Gas chromatography analysis

In this study, GC was used to analyze the decomposition products of target gases. GC analysis was performed on an HP 5890 chromatograph, whose injection port (maintained at 100 °C) was connected with a pulse micro-reactor (6 mm in diameter and 25.4 cm in length). The other port of the HP 5890 chromatograph was connected with a Porapak-Q column (3.2 mm in diameter and 180 cm in length) to separate the output components, which was connected with a thermal conductivity detector (maintained at 200 °C). The calcined and ball milled SnO<sub>2</sub>-based powder (100 mg) was placed in the middle of the micro-reactor, where target gases passed through. The measurements were carried out in a humid air atmosphere, which is the same condition of general operation of a sensor. Helium gas was also used as a carrier gas with a flow rate of 2.0 ml·minute<sup>-1</sup> to maintain the retention time of the air peak at 0.9 minute. Chromatograms measured at various experimental conditions were obtained. Using the retention times (RTs) of expected decomposition products determined beforehand, the type of decomposed gases were identified. The quantitative amount of each gas produced was obtained by the integration of the area of each peak.

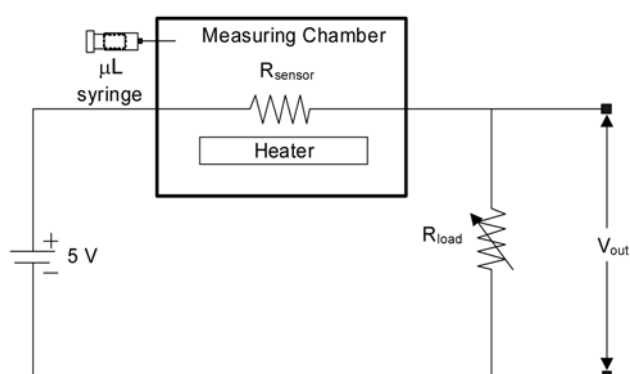


Fig. 2. Schematic circuit diagram for the measurement of the sensor resistance.

### Characterization of gas sensing properties

The gas sensing properties of the assembled sensors (Fig. 1) were measured using previously described procedures [13]. The concentrations of target gases (100 ppm) were controlled by the injection of each target gas into a polycarbonate chamber (60 l) equipped with a built-in fan and a heater. The injected solvents were completely vaporized on a hot glass plate (about 75 °C). The injection volume ( $V_i$ ) was calculated for the evaluation of gas concentration ( $c$  in ppm) by:

$$V_i(\mu\text{l}) = \frac{c(\text{ppm}) \cdot V_{\text{Box}}(\text{l}) \cdot MW(\text{g/mol}) \cdot 10^{-3}}{22.45(\text{l/mol}) \cdot D_i(\text{g/ml}^3)} \quad (1)$$

where, the gas constant (22.45 l/mol) means the volume of 1 mol gas at 1 atm, MW denotes the molecular weight of the injected gas, and  $D_i$  is the density of the injected sample.

The operating temperature of the sensors was varied from 150 to 450 °C. The sensitivity ( $S$ ) of the sensors was defined as  $(R_a/R_g) \times 100$  (%), where  $R_a$  and  $R_g$  are the resistances in air and the gas, respectively. The measuring circuit for the sensor resistance used in this study is schematically illustrated in Fig. 2. The powdered sample and the thick films were heated at 300 °C for 72 h in air for stabilization prior to the measurement of gas sensing and the GC analysis.

## Results

### Electrical resistances

At the operating temperature of 150–500 °C in atmosphere, oxygen atoms are adsorbed onto the SnO<sub>2-x</sub> surface by capturing electrons from the conduction band and remain as O<sub>ads</sub><sup>-</sup> [7, 8, 14] until they are desorbed. This process can be expressed as follows:



which increases the resistance of the sensors. In addition, the main effect of the additives introduced is the variation of the electrical properties resulting from the

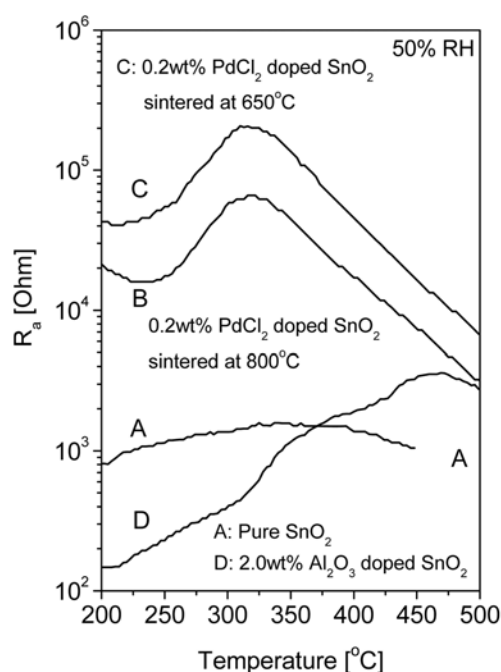


Fig. 3. Variation of sensor resistances with temperature.

modification of surface conditions. The additives result in a higher density of surface adsorption sites, which induces higher oxygen adsorption at the grain surfaces and increases the grain barriers. Also, the presence of noble metallic clusters localized at the grain surfaces can induce higher oxygen adsorption at the grain surfaces. Such effects can be seen in Fig. 3.

Shown in Fig. 3 is the variation of the resistance of pure and doped SnO<sub>2</sub> elements with temperature in the humid air atmosphere. The resistance measurements in this study were carried out in a humid air atmosphere of 50% relative humidity because water vapor in air markedly influences the electrical properties of sensor elements as a consequence of dissociation and reduction processes. The resistance of an undoped SnO<sub>2</sub> element at room temperature was around 630 Ω. The resistance of doped SnO<sub>2</sub> elements, however, showed higher values due to the increase of the grain barriers resulting from the modification of the surface conditions by additives. Such an effect is evident in the SnO<sub>2</sub> sensor element doped with palladium. As can be seen in Fig. 3, the peak resistance showing a maximum resistance in the Pd-doped SnO<sub>2</sub> (SnO<sub>2</sub>:Pd) elements was found at 325 °C. The 650 °C-sintered SnO<sub>2</sub>:Pd elements containing 0.2 wt% PdCl<sub>2</sub> showed higher resistances than those of the same elements sintered at 800 °C. By contrast, the maximum resistance of the Al-doped SnO<sub>2</sub> (SnO<sub>2</sub>:Al) elements was found at 460 °C. The resistances of SnO<sub>2</sub>:Al elements at 200 °C was even decreased compared with those of pure SnO<sub>2</sub>, which may be due to the effect of Sn substitution for Al ions at high temperature.

### Gas sensing properties

The SnO<sub>2</sub>-based elements, both pure and doped with foreign metals such as Pd, Al, and La, were subjected to gas sensing experiments. The amount of PdCl<sub>2</sub>, Al<sub>2</sub>O<sub>3</sub> and La<sub>2</sub>O<sub>3</sub> was 0.25-1.0, 2.0, and 5.0 wt%, respectively, all of which was approximately below the order of one monolayer coverage of a SnO<sub>2</sub> surface if the dopants were assumed to spread uniformly over the SnO<sub>2</sub> grains.

For the detection of alcohol gases with the SnO<sub>2</sub>-based sensor elements, it is well-known that chemisorbed oxygen at SnO<sub>2</sub> surfaces plays an important role. As a result of chemisorption there can appear O<sup>2-</sup>, O<sub>2</sub><sup>-</sup>, and O<sup>-</sup> ions depending on the temperature at the surface of transition-metal oxides [8, 15, 16], whose coverage at the surface is restricted by the Weisz limit [17]. Among them O<sub>2</sub><sup>-</sup> is classified as an 'electrophilic' agent while O<sup>-</sup> connected with the lattice at the surface as a 'nucleophilic' agent [18]. According to Kohl [8], O<sub>2</sub><sup>-</sup> species are highly unstable and do not play much role in determining the sensitivity. Meanwhile, O<sup>-</sup> species were reported to be highly active and dominant in SnO<sub>2</sub> at the temperatures range between 423 and 933 K [18, 19]. Thus, the major adsorbed species that influences the sensitivity of a sensor element might be O<sup>-</sup>. This adsorbed oxygen creates a space charge region near the film surface by extracting electrons from the material. Ethanol, being reducing in nature, removes adsorbed O<sup>-</sup> species from the surface and re-injects the electrons back to the material, thereby reducing the resistance.

Upon exposure to 100 ppm of alcohol gas, the electric resistance R<sub>a</sub> of each sensor element in air decreased to a new value R<sub>g</sub>. The gas sensitivity  $S (R_a/R_g)$  is plotted against temperature (200-450 °C) in Figs. 4 for ethanol gas and 5 for methanol gas. The gas sensitivity of the pure SnO<sub>2</sub> sensors to the reducing gases is generally maximized at the operating temperature range of 300-350 °C, below and above which the gas sensitivity decreases [20-23]. At the lower operating temperature range of 100-300 °C, the desorption of water and adsorption of oxygen ions (mainly O<sub>ads</sub><sup>-</sup> ions) dominates, which increases the resistance as well as the gas sensitivity. Moreover, the reduced activation energy for the chemical reaction between the reducing gases and the surface-adsorbed oxygen ions (mainly O<sub>ads</sub><sup>-</sup> ions) favors higher gas sensitivity with increasing operating temperature. On the other hand, in the higher operating temperature range of 350-500 °C, the desorption of the surface-adsorbed oxygen ions dominates, which reduces the film resistance and the gas sensitivity with increasing operating temperature [24]. Also, the microstructural changes such as grain growth may reduce the gas sensitivity within the higher operating temperature range (350-500 °C) due to a decrease of surface area.

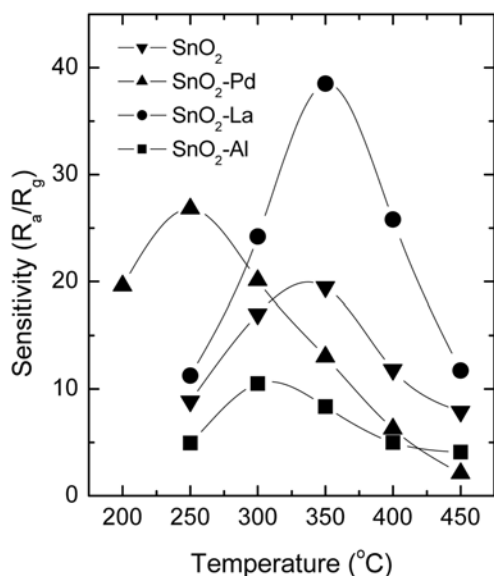


**Fig. 4.** Sensitivity vs. temperature relationship for the SnO<sub>2</sub>-based sensors to 100 ppm ethanol.

The addition of foreign atoms induced marked influences in sensitivity. The maximum of the sensitivity of pure and SnO<sub>2</sub>:La was observed at about 350 °C as shown in Fig. 4, while the maximum sensitivity of SnO<sub>2</sub>:Pd was found at 250 °C. The addition of basic La<sub>2</sub>O<sub>3</sub> leads to a prominent increase of the sensitivity to ethanol over the entire temperature range, which is due to a relatively higher conversion yield of ethanol through oxidative dehydrogenation [13]. The maximum sensitivity temperature of La-doped SnO<sub>2</sub> was, however, not changed compared with that of pure SnO<sub>2</sub>. In contrast, the sensitivity of acidic Al<sub>2</sub>O<sub>3</sub>-doped SnO<sub>2</sub> to ethanol was suppressed. This appears to be related with the preferential dehydration of ethanol when passed over SnO<sub>2</sub>:Al, which would consume the weakly-adsorbed oxygen species ( $O_{ads}^-$ ) and result in a declined sensitivity [12]. Also, we observed a slight shift of the maximum sensitivity to a lower temperature. In the case of SnO<sub>2</sub>:Pd, the presence of Pd catalyst in the sensor provided sites for co-adsorption of oxygen and reducing gas, which increased the rate of adsorption. The SnO<sub>2</sub>:Pd sensor showed a peak sensitivity at 250 °C, which is significantly lower than that of the undoped SnO<sub>2</sub> with a peak at 350 °C. Palladium is known to exist mainly as PdO or PdO<sub>2</sub>, an ample source of oxygen [11, 25]. According to Kohl [26], the formation of the C–C bond cleavage product (CH<sub>4</sub>), which requires the consumption of the adsorbed oxygen ( $O_{ads}^-$ ), might be promoted by the addition of palladium, which will be discussed later.

For methanol gas, similar gas sensing behaviors were observed. The SnO<sub>2</sub>:Pd showed an enhanced sensitivity at temperatures below 250 °C, as shown in Fig. 5. This seems closely related to the oxidation products (see next section), *i.e.*, CO and CO<sub>2</sub>, which consume  $O_{ads}^-$

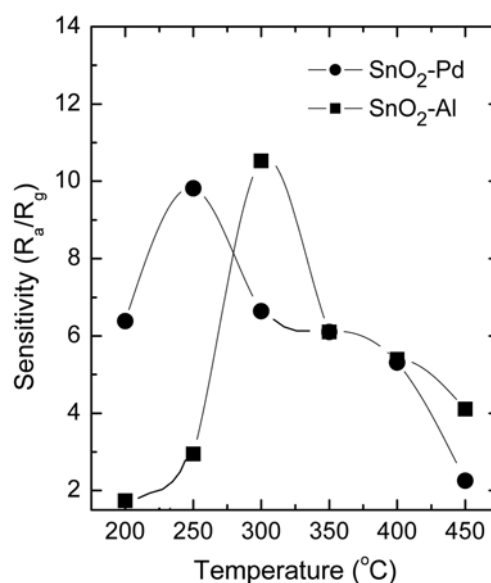


**Fig. 5.** Sensitivity vs. temperature relationship for the SnO<sub>2</sub>-based sensors to 100 ppm methanol.

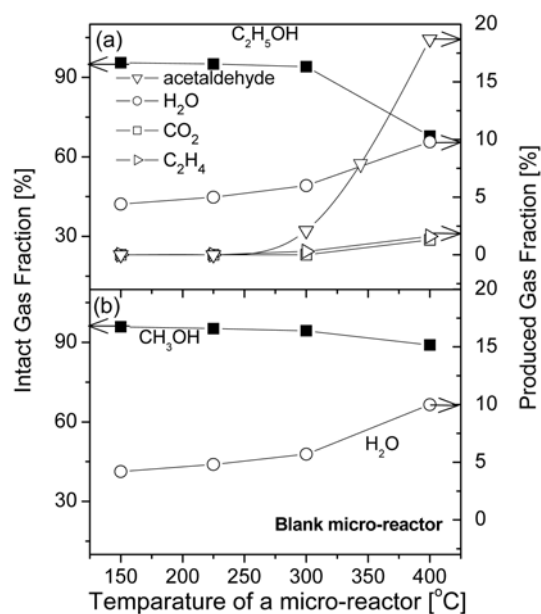
at low temperatures. The sensitivity of the SnO<sub>2</sub>:Al showed a peak value at 300 °C and then decreased at temperatures below 300 °C. This might be related with the preferential dehydration process seen when methanol is passed over the Al<sub>2</sub>O<sub>3</sub>-doped SnO<sub>2</sub> at 150 °C and the increased catalytic oxidation at 300 °C. At higher temperatures, as was seen with ethanol, a faster combustion at the SnO<sub>2</sub> surface would depress the sensitivity.

### Thermal decomposition behaviors

GC is an analytical technique which makes it possible to separate gas mixtures into individual gas components qualitatively on the basis of differences in vapor pressure and interaction with the other phases. For this reason, GC was used in this study as an analytical tool to investigate the decomposition products of alcohol gases including ethanol (C<sub>2</sub>H<sub>5</sub>OH) and methanol (CH<sub>3</sub>OH). Once the target gas is injected into a micro-reactor connected with a chromatograph, it decomposes depending on the temperature and the presence of sensor elements inside the micro-reactor. The decomposition products as well as the intact target gas will pass through the measurement system by the gas flow (2.0 ml/minute<sup>-1</sup>) of helium carrying gas. In this case, the required time for each gas before detection should be different because the gases have different molecular weights. Thus, retention time, meaning the time required for a solute to travel through the Porapak Q column before detection, can serve as a reference in analyzing the generated reaction products. To analyze the reactions between various injected target gases and the SnO<sub>2</sub> sensors, the retention time of the expected products such as CO, methane (CH<sub>4</sub>), CO<sub>2</sub>, ethylene (C<sub>2</sub>H<sub>4</sub>), H<sub>2</sub>O, formic acid (HCOOH), and acetaldehyde (CH<sub>3</sub>CHO) were measured beforehand and are indicated in Table 1.

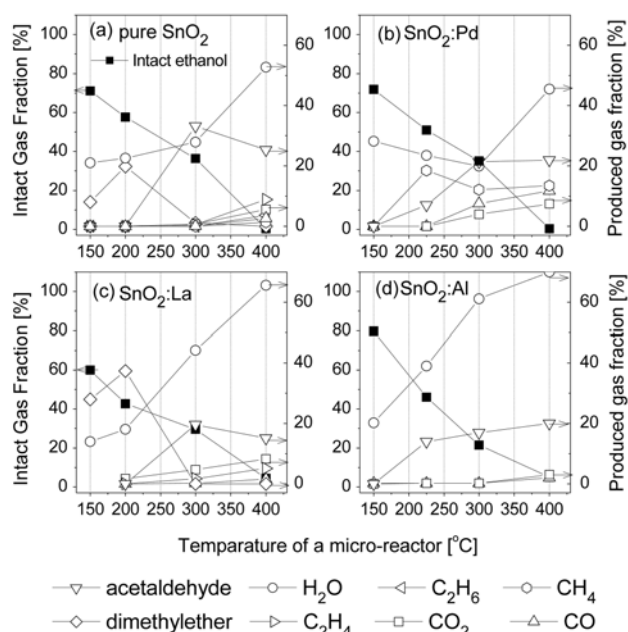
**Table 1.** Retention time (RT) of possible reaction products generated during the reaction of gases and sensor powders

Components	CO	methane (CH <sub>4</sub> )	CO <sub>2</sub>	ethylene (C <sub>2</sub> H <sub>4</sub> )	H <sub>2</sub> O	formic acid (HCOOH)	acetaldehyde (CH <sub>3</sub> CHO)
RT [minutes]	0.9	1.1	1.2	1.6	2.5	2.8	7.0

**Fig. 6.** Variations of decomposition products of ethanol (a) and methanol (b) in a blank micro-reactor with temperature.

First, 0.1  $\mu\text{l}$  of each target gas was injected individually into a blank micro-reactor and then each chromatogram, expressed as retention time and peak area ratios, was obtained. Figure 6 shows the decomposition behavior of alcohol gases injected into a blank micro-reactor in the temperature range of 150–400 °C. As shown in Fig. 6(a), ethanol slightly decomposed forming H<sub>2</sub>O as a major decomposition product up to 300 °C. Ethanol started to decompose at a temperature above 350 °C, generating acetaldehyde (CH<sub>3</sub>CHO) and water as the major products. At 400 °C, the major decomposition products of ethanol were acetaldehyde (18.7%), H<sub>2</sub>O (9.8%), C<sub>2</sub>H<sub>4</sub> (1.6%), CO<sub>2</sub> (1.3%), C<sub>2</sub>H<sub>6</sub> (0.6%), and intact ethanol (67.8%). Meanwhile, methanol was slightly decomposed up to 400 °C, as shown in Fig. 6(b), meaning the decomposition was not accelerated with an increase of micro-reactor temperature up to 400 °C.

For the analysis of the thermal decomposition behaviors of alcohol gases in the presence of the doped SnO<sub>2</sub>-based sensor material (100 mg), GC experiments were performed using the same experimental conditions after locating the doped SnO<sub>2</sub> powders in the middle of a micro-reactor. The SnO<sub>2</sub> sensor materials tested were Pd-, Al-, and La-doped SnO<sub>2</sub> powders which were produced under the same conditions with the screen printed elements. By injecting alcohol gases into the micro-reactor, the effect of dopants on the

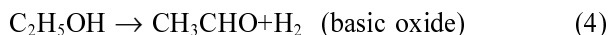
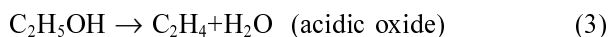
**Fig. 7.** Variations of decomposition products of ethanol in a SnO<sub>2</sub> loaded micro-reactor with temperature: (a) pure SnO<sub>2</sub>, (b) SnO<sub>2</sub>:Pd, (c) SnO<sub>2</sub>:La, and (d) SnO<sub>2</sub>:Al.

thermal decomposition behavior of alcohol was characterized.

Figure 7 indicates the thermal decomposition behavior of the injected ethanol (0.4  $\mu\text{l}$ ) monitored at a reactor temperature range of 150–400 °C when it passed through a micro-reactor containing SnO<sub>2</sub>-based sensors containing Pd-, Al-, and La-additives. The presence of the SnO<sub>2</sub>-based elements generally accelerated the decomposition of the target gases. In particular, the presence of 1.0 wt% PdCl<sub>2</sub>-added SnO<sub>2</sub> greatly enhanced the decomposition of injected gases at lower temperatures due to the catalytic effect of Pd on the surface reactions of the SnO<sub>2</sub> surface. When 1.0 wt% PdCl<sub>2</sub>-added SnO<sub>2</sub> elements were used, acetaldehyde (CH<sub>3</sub>CHO) and additional decomposition products such as methane (CH<sub>4</sub>) were found. Ethanol rapidly decomposed to H<sub>2</sub>O, CO<sub>2</sub>, and CO at 300 °C so that the intact ethanol fraction at 300 °C was only 50 %. The decomposition of methanol was also accelerated in the presence of 1.0 wt% PdCl<sub>2</sub>-added SnO<sub>2</sub> forming H<sub>2</sub>O, CO<sub>2</sub>, CO, and CH<sub>4</sub>. When the SnO<sub>2</sub> powder doped with 2.0 wt% Al<sub>2</sub>O<sub>3</sub> was used, the amount of decomposition products were increased as the temperature of the micro-reactor increased up to 300 °C. Similar to the case of PdCl<sub>2</sub>-added SnO<sub>2</sub> powders, the amount of decomposition products were increased as the temperature of the micro-reactor increased up to 300 °C. The observed decom-

position behavior of  $C_2H_5OH$  in the presence of  $Al_2O_3$ -added  $SnO_2$ , however, showed quite different results compared with that observed in  $PdCl_2$ -added  $SnO_2$ . A considerable amount of methane produced during the reaction between  $C_2H_5OH$  and  $PdCl_2$ -doped  $SnO_2$  was not observed. Instead, a large amount of  $H_2O$  and a small amount of ethylene ( $C_2H_4$ ) were observed. This means that a different decomposition reaction step would take place at the  $SnO_2$  surfaces depending on the type of additives. When the  $SnO_2$  powder doped with 1.0 wt%  $La_2O_3$  was used, the decomposition was also accelerated.

It is well-known that either methanol ( $CH_3OH$ ) or ethanol ( $CH_3CH_2OH$ ) is initially adsorbed on the surface of  $SnO_2$  as a form of methoxide ( $OCH_3$ ) or ethoxide ( $OC_2H_5$ ), respectively [7, 17]. In particular, it has been reported that ethanol gas undergoes two routes of decomposition reactions, i.e., dehydration and oxidative dehydrogenation at elevated temperature, depending on the acid-base properties of the oxide catalysts doped [7, 17, 27]:



According to the literature data, ethanol experiences two different reaction steps [8] depending on the type of catalyst. When an acidic catalyst (e.g.  $Al_2O_3$ ) is added into  $SnO_2$ , ethanol decomposes forming ethylene ( $C_2H_4$ ) after the initial dehydration step. When a basic catalyst (e.g.  $La_2O_3$ ) is added, however, acetaldehyde ( $CH_3CHO$ )

is also observed as a major intermediate form of ethanol after the initial dehydrogenation.  $CH_3CHO$  is known to have a much higher molecular sensitivity to a semiconductor gas sensor than  $C_2H_4$  [28]. Dehydration usually takes place at lower temperatures compared with dehydrogenation. In this study, both  $CH_3CHO$  and  $C_2H_4$  were observed in all cases except for  $Pd$ -doped  $SnO_2$ , which means that  $SnO_2$  has both acidic and basic characteristics. Meanwhile, when  $PdCl_2$  catalyst is added, ethanol was found to experience an intermediate step of  $CH_3CHO$  formation instead of  $C_2H_4$ . Furthermore such dehydration happened at a lower temperature of  $150^\circ C$  compared with the other cases. At the same time, the formation of methane ( $CH_4$ ) as a decomposition product was also observed, which means that  $Pd$  catalyst played an important role in the surface reaction. Considering the decomposed products of  $CO$ ,  $CO_2$ , and  $H_2O$  (see Fig. 8) observed in this study, methanol decomposes to an intermediate methoxide and then reacts with adsorbed oxygen at the surface of  $SnO_2$ , regardless of the type of additive used in this study. In this study, ketene ( $C_2H_2O$ ) having a high reactivity was not observed through the decomposition reaction.

## Discussion

When target gas molecules are brought into contact with the sensing element, high-reactivity intermediate species such as dissociated atoms, free radicals, electrons, and excited molecules are formed. These species react with the adsorbed oxygen at the surface of a sensor element, which induces conductance variation. Depending on the extent of such variations over the specific gases, the sensing characteristics of the sensor elements are determined. To enhance the sensing characteristics and the speed of response of a sensor material to a specific gas, transition metals or metal ions acting as catalysts are added. Upon exposure to the sensing element containing catalysts, such intermediate species are preferably adsorbed on the catalysts distributed at the surface of sensor elements. Then, the intermediate species move on the surface or into the bulk of the sensor materials before recombination with either pre-adsorbed species on the surface or other defects in the bulk phase. This movement happens due to a gradient in electrochemical potential between the activation site and the recombination site of the intermediate species. The recombination with other active species will complete the process of exchanging electrons between the sensing elements and the gas to be detected. Generally, the overall reaction mechanism between the sensor element and the gas to be detected is complicated due to the complex reaction among the intermediate species, the sensor materials, and the catalysts. Based on the GC qualitative study, we further investigated the reaction mechanism between the sensor element and the target gas for the elucidation of the complete reaction.

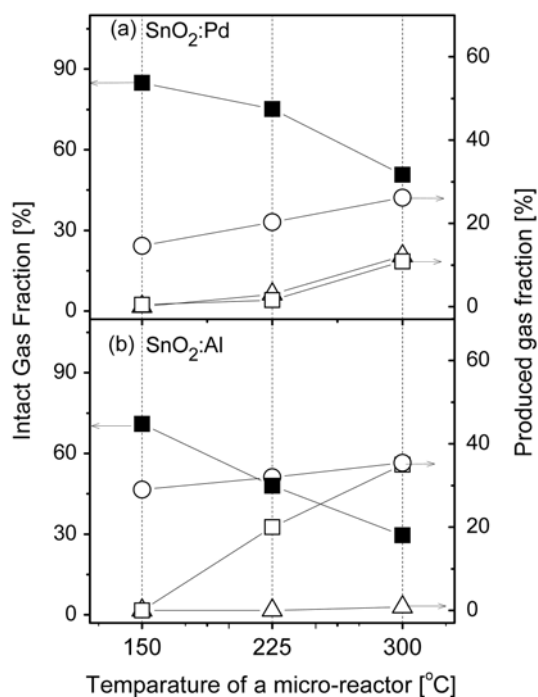
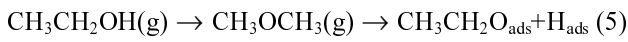


**Fig. 8.** Variations of decomposition products of methanol in a  $SnO_2$ -loaded micro-reactor with temperature: (a)  $SnO_2$ :Pd, and (d)  $SnO_2$ :Al.

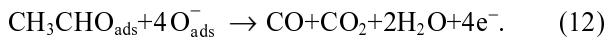
When ethanol is injected into the micro-reactor containing either pure SnO<sub>2</sub> compound or SnO<sub>2</sub>:La, a large fraction of ethanol was found to be transformed to dimethylether (CH<sub>3</sub>OCH<sub>3</sub>) below and at 200 °C (see Fig. 7a and c). It then may be adsorbed in the form of ethoxide (CH<sub>3</sub>CH<sub>2</sub>O) producing an adsorbed hydrogen atom. At about 300 °C, this transformed to acetaldehyde (CH<sub>3</sub>CHO) forming an adsorbed hydrogen atom. The adsorbed hydrogen atoms then loose electrons to the conduction band of SnO<sub>2</sub>. The generated protons (H<sup>+</sup>) get associated with the surface-adsorbed oxygen ions forming OH<sub>ads</sub>. These two adsorbed OH groups condense and eliminate H<sub>2</sub>O leaving an adsorbed oxygen. During the above dehydrogenation process, one net electron is released into the conduction band of SnO<sub>2</sub> reducing its resistance. The overall dehydrogenation process is summarized as follows:



The net reaction is:



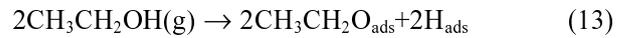
The adsorbed acetaldehyde (CH<sub>3</sub>CHO<sub>ads</sub>), an intermediate compound, is then decomposed to CO, CO<sub>2</sub>, and H<sub>2</sub>O by the following reaction:



Both pure SnO<sub>2</sub> and SnO<sub>2</sub>:La showed similar ethanol decomposition behaviors. A distinctive difference was the amount of initial dimethylether produced at a lower temperature, which was due to the catalytic effect of La. The active transformation of ethanol to dimethylether in SnO<sub>2</sub>:La may be attributed to the higher sensitivity to ethanol. Also, the decomposition of acetaldehyde (Eq. 12) at and above 300 °C was more active in the SnO<sub>2</sub>:La compared with that in the pure SnO<sub>2</sub>, which also can be attributed to the higher sensitivity to ethanol. Lanthanum has been known to enhance the properties of a SnO<sub>2</sub> sensor for the following two reasons: A basic oxide such as La<sub>2</sub>O<sub>3</sub> introduced in the SnO<sub>2</sub> matrix will promotes the basicity of the surface such that the dehydrogenation route is more favored than the hydration one and consequently the ethanol sensitivity increases. The other reason for the improvement of ethanol sensitivity of the SnO<sub>2</sub> sensor element is the increasing surface area due to the decreasing crystallite size when the La dopant concentration rises. The same effect has been reported by Xu et al. [29]. Above 3 at.% La, however, the solubility limit is reached and a

secondary phase of La<sub>2</sub>O<sub>3</sub> precipitates on the surface leading to its inhomogeneity and poor ethanol sensitivity. With an increase of the dopant concentration, the surface becomes more basic and with finer crystallites, which promotes the sensitivity. On the other hand, the appearance of precipitates leads to a deterioration of the surface quality and consequently decreases the ethanol sensitivity and makes the response time longer above 3 at.% La introduced in the films.

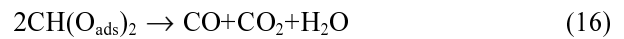
Meanwhile, when ethanol is injected into a micro-reactor containing the SnO<sub>2</sub>:Pd, a considerable amount of CH<sub>4</sub> was detected from the low operating temperature instead of the formation of dimethylether. Especially, at 225 °C, the fraction of CH<sub>4</sub> was 18.5%, which is a much higher amount compared to that (1.3%) decomposed from the pure SnO<sub>2</sub> at 400 °C. According to Kohl [26], when no adsorbed oxygen is present, the CH<sub>4</sub> formation accompanies the formation of oxygen vacancies. In our case, however, there should be lots of adsorbed surface oxygen due to the migration (or spillover) of adsorbed oxygen from the metal catalyst particles onto the SnO<sub>2</sub> surface [30]. Thus, when ethanol is injected into a reactor containing the SnO<sub>2</sub>:Pd, the adsorbed ethoxide (see Eq. 5) react directly with adsorbed oxygen and form CH<sub>3</sub>CO<sub>(ads)</sub>O<sub>(ads)</sub> instead of the formation of acetaldehyde (see Eq. 5 and Fig. 7(b), where no acetaldehyde was detected), which can be expressed as:



Also, the intermediate compound further decomposed forming methane (CH<sub>4</sub>) according to the following reaction:



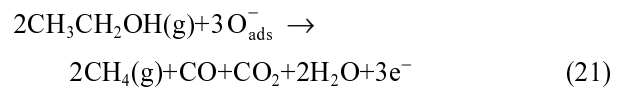
Finally, CH<sub>3</sub>CO<sub>ads</sub>O<sub>ads</sub> decomposed to CO, CO<sub>2</sub>, and H<sub>2</sub>O as follows:



In addition, the adsorbed hydrogen atom forms H<sub>2</sub>O in the previously described manner:



The net reaction is:



which increases the free electron concentration. The mechanism of alcohol sensing in the presence of SnO<sub>2</sub>:Pd is schematically illustrated in Fig. 9. Because there should be lots of surface-adsorbed oxygen ions



17. P.B. Weisz, *J. Chem. Phys.* 21 (1953) 1531-1538.
18. A. Bielaski, and J. Haber. *Catal. Rev. -Sci. Eng.* 19 (1979) 1-6.
19. N. Yamazoe, J. Fuchigami, M. Kishikawa, and T. Seiyama, *Surf. Sci.* 86 (1979) 335-344.
20. V. Jayaraman, K.I. Gnanasekar, E. Prabhu, T. Gnanasekaran, and G. Periaswami, *Sens. Actuators B* 55 (1999) 147-153.
21. G. Zhang, and M. Liu, *Sens. Actuators B* 69 (2000) 144-152.
22. A. Carbot, J. Arbiol, J.R. Morante, W. Weimar, N. Barsan, and W. Göpel, *Sens. Actuators B* 70 (2000) 87-100.
23. S.-S. Park, and J.D. Mackenzi, *Thin Solid Films* 274 (1996) 154-159.
24. N.S. Baik, G. Sakai, N. Miura, and N. Yamazoe, *Sens. Actuators B* 63 (2000) 74-79.
25. S. Matsushima, Y. Teraoka, N. Miura, and N. Yamazoe, *Jpn. J. Appl. Phys.* 27 (1988) 1798-1802.
26. D. Kohl, *J. Phys. D: Appl. Phys.* 34 (2001) R125-R149.
27. D. Kohl, *Sens. Actuators* 18 (1989) 71-113.
28. I. Stambolova, K. Konstantinov, S. Vassilev, P. Peshev, and Ts. Tsacheva, *Mater. Chem. Phys.* 63 (2000) 104-108.
29. C. Xu, J. Tamaki, N. Miura, and N. Yamazoe, *Chem. Lett.* (1990) 1143-1145.
30. G. Korotcenkov, V. Brinzari, Y. Boris, M. Ivanov, J. Schwank, and J. Morante, *Thin Solid Films* 436 (2003) 119-126.